Finite Element Model for Simulating the Inspection of Steel Tubes Using Electromagnetic Acoustic Transducers

Pengfei Sun*, Xu Ding, Xinjun Wu and Ming Cong
School of Mechanical Science & Engineering, Huazhong University of Science and Technology, Wuhan 430074, China.
* Corresponding author: hustpfs@gmail.com

Abstract : Steel tubes are widely used in industries. In order to ensure the safety and reliability of industrial processes, electromagnetic acoustic transducers (EMATs) based guided wave technology have been developed for inspecting stainless steel tubes regularly. Theoretical models and finite element modes have been built to investigate the EMAT technology. However, existing models mainly focused on studying the transmitting process of the EMAT. In this paper, we present a finite element model, using COMSOL Multiphysics, to simulate the whole process of inspecting stainless steel tubes using EMATs, including both the transmitting and receiving processes.

Keywords : Electromagnetic acoustic transducers, nondestructive testing, tube, finite element model.

1. Introduction

Steel tubes are key element in the area of energy industries. Corrosions and rusting may occur on them mainly because of the working environment they exist, which finally will due to the fracture of tubes and the leak of the materials in them. The fracture of tubes may do great harm to the economic benefit and the social security. Therefore, it is of great importance to inspect steel tubes regularly.

There are many methods for inspecting steel tubes, such as, the eddy current testing, the magnetic flux leakage and the ultrasonic waves, and the guided waves testing (GWT)[1]. Compared with other technologies, GWT has a distinct advantage of high detection efficiency, due to its ability of scanning the whole tube without pulling the transducer through the length of the tube. It means that, by applying GWT, the detection efficiency for inspecting steel tubes can be greatly improved.

Electromagnetic acoustic transducers (EMATs) have been widely used for inspecting steel tubes. The EMATs can generate guided waves in the steel tubes without physical contacts as they work on the coupling between alternating magnetic fields and the static magnetic field in the tubes[2]. Due to this advantage, EMATs are more suitable for the online inspection of steel tubes. However, compared with the conventional piezoelectric sensors, another approach for generating guided waves, EMATs show relatively low transduction efficiency which is in direct proportion to the sensitivities of defects in the tubes.

To improve the transduction efficiency of the EAMTs, existing methods mainly focus on optimizing the structure of EMATs, used as a transmitter, based on theoretical models or finite element models. However, the receiving process of the EMAT is also as important as the generating process. The transduction efficiency would also be improved by optimizing the structure of EMATs used as a receiver.

The previous work[3] of the authors has investigated the effect of the magnetic core on the transmitting efficiency of the EAMT which is used for generating guided waves of L(0,1) mode. Here, a further work is carried out that the influence of the magnetic core on the receiving efficiency is studied. A finite element (FE) model is presented which consists of the receiving processes of the EMAT, based on COMSOL Multiphysics. The received signals obtained under cores with different materials are simulated based on the FE model. The optimal material of the core under which the maximal transmitting efficiency are obtained is then chosen for the EMAT as a receiver.

2. Structure of the EMAT

The structure of the EMAT, which is used to generate and receive guided waves of longitudinal modes for inspecting steel tubes, is shown in Fig.1. Magnetizers which consist of back irons and permanent magnets are placed on the tube and produce uniform axial static magnetic fields in the tube. Solenoid coils are wound on the tube and used as the transmitter or the receiver coils. When the EMAT is used as a transmitter, the coil generates a dynamic magnetic field in the tube. Axial strain is induced in the skin area of the tube by the coupling between two magnetic fields based on the magnetostriction effect. Then guided waves are generated by the axial stain and propagates along the tube axis. When guided waves pass through the area where the static magnetic field induced by the receiver exists, an induced magnetic field will be generated. The time-dependent magnetic flux in the cross section area of the receiver coil is turned into induced voltages based on Faraday's law.

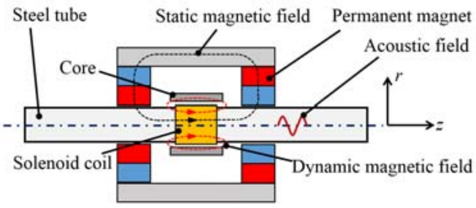

Fig.1 The structure of the EMAT for generating and receiving guided waves of longitudinal modes. When the EMAT is used as a transmitter, the dynamic magnetic field is generated by the coil. When the EMAT is used as a receiver, the dynamic magnetic field is induced by the elastic waves path through the EMAT.

3. The FE model

It can be seen that the receiving process is the coupling process between the elastic field and the magnetic field. When the bias magnetic field is much stronger than the alternating magnetic field, the magnetostriction is linear. As the static magnetic field is uniform in the area where the coil works, the magnetostriction coefficient can be seen as the same. The coupling of the elastic field and the magnetic field can be described by [4]:

$$\nabla\times\left(v\nabla\times\mathbf{A}\right)-\sigma\frac{\partial\mathbf{A}}{\partial t}=\mathbf{J}_L+\mathbf{J}_{mz}+\mathbf{J}_{ms} \tag{1}$$

$$\mathbf{J}_L=\sigma\frac{\partial\mathbf{u}}{\partial t}\times B_0 \tag{2}$$

$$\mathbf{J}_{mz}=-\nabla\times(M_0\nabla\cdot\mathbf{u}) \tag{3}$$

$$\mathbf{J}_{ms}=Kve^{ms}\varepsilon \tag{4}$$

where A is the magnetic vector potential. σ is the conductivity of the tube. $\mathbf{J}_L$, $\mathbf{J}_{mz}$ and $\mathbf{J}_{ms}$ are the Lorentz current density, the magnetization current density and the magnetostrictive current density induced by the elastic waves which pass through the EMAT, respectively. **u** is the displacement vector of a particle. B_0 is the static magnetic field density. M_0 is the static magnetization. e^{ms} is the inverse dynamic magnetostriction matrix. v is the inverse magnetic conductivity matrix. ε is the stain caused by the elastic waves.

In the coupling relationship, the displacement **u** and the stain ε can be calculated in the solid mechanics interface. The sum of $\mathbf{J}_L$, $\mathbf{J}_{mz}$ and $\mathbf{J}_{ms}$ is applied on the tube area and used as an input of a magnetic field interface. The induced voltage of the receiver coil is the final output of the whole model. The details of the FE process are show in Fig.2. The schematic diagram of the FE model is shown in Fig.3.

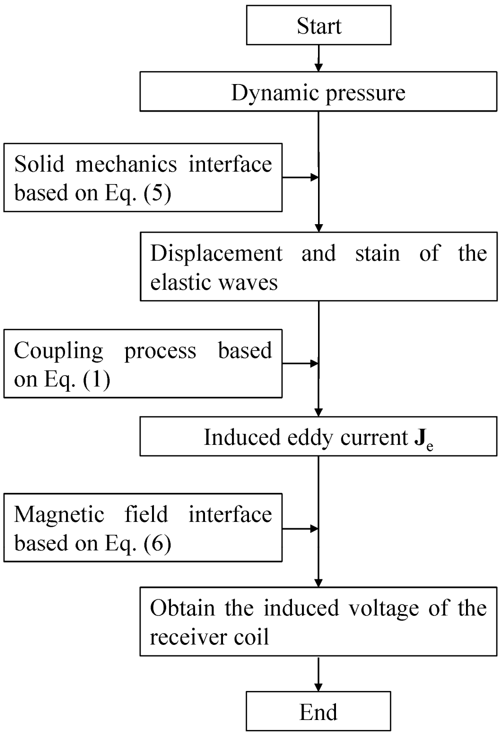

Fig.2. Process of the finite element analysis.

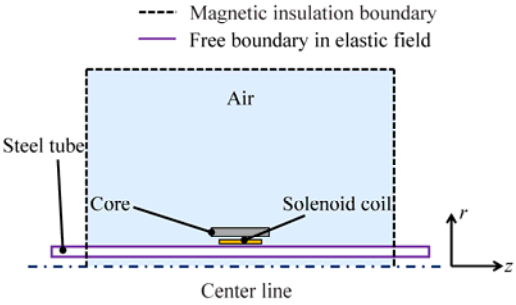

Fig.3. Schematic diagram of the FE model.

Firstly, a four-cycle hanning windowed pressure at a frequency of 30 kHz with an amplitude of 1 Pa is applied on the tube, as shown in Fig.4. The elastic field is calculated through:

$$\rho \frac{\partial^2 \mathbf{u}}{\partial t} - \nabla \cdot \sigma = \mathbf{F}_V \tag{5}$$

where ρ is the density of the tube. $\mathbf{F}_v$ is the body force. The longitudinal waves generated by the pressure is show in Fig.5. Induced eddy currents are calculated based on Eqs.(1)-(4) based on the displacements and the strain. Then the eddy currents are used as an input of the magnetic field interface. The dynamic magnetic field generated by the elastic waves are obtained based on:

$$\sigma \frac{\partial \mathbf{A}}{\partial t} + \nabla \times \mathbf{H} = \mathbf{J}_e \tag{6}$$

where $\mathbf{H}$ is the magnetic field strength. $\mathbf{J}_e$ can be seen as the sum of $\mathbf{J}_L$, $\mathbf{J}_{mz}$ and $\mathbf{J}_{ms}$, which is applied on the tube area where the EMAT works.

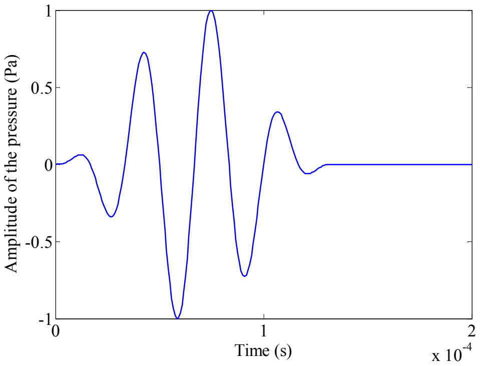

Fig.4 The dynamic pressure applied on the tube.

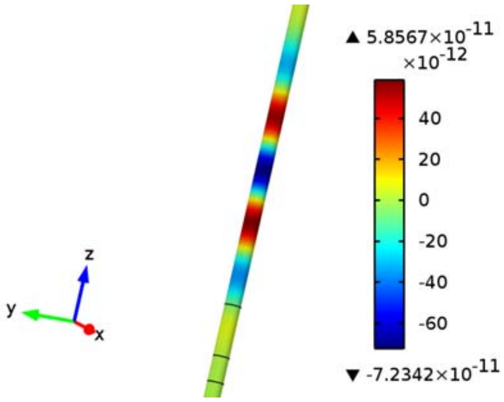

Fig.5 The longitudinal waves generated in the tube.

The strength of the induced magnetic field when the elastic waves pass through the tube where the EMAT exists is shown in Fig.6. As the elastic waves propagates along the tube, the induced magnetic field also moves which due to the change of the magnetic flux in the coil. Finally, the induced voltage is obtained.

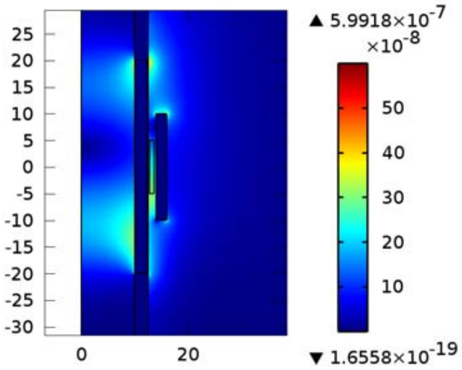

Fig.6. The strength of the induced magnetic field.

Table.1 The materials of different cores used here

Material of the core	*Equivalent* $\mu_r$$^{(5)}$	$\sigma^{(5)}$ (S/m)
Permalloy	650	1.67e6
Mn-Zn ferrite	400	1
Ni-Zn ferrite	300	2e-3
Air	1	0

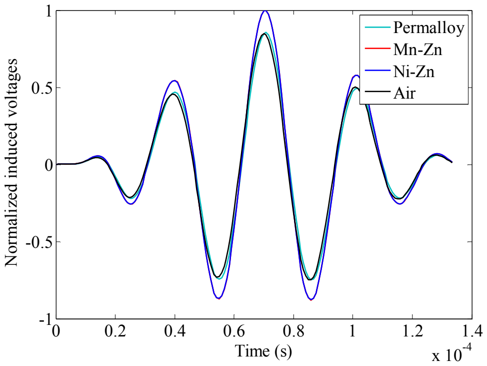

Fig. 7 The induced voltages obtained under cores with different materials

4. Results and Discussions.

For a detailed investigation on the influence of the core, three cores with different materials but the same size are used, the permalloy, the Mn-Zn ferrite and the Ni-Zn ferrite. The equivalent relative permeability is calculated based on the

B-H curve and the static magnetic field. The induced voltages are simulated under four different conditions that three cores with different materials are used and no core are used (air). The detailed equivalent relative permeability and the conductivity of four conditions in the simulations are shown in Table 1. The induced voltage of the receiver coil obtained under four conditions are shown in Fig.7. It can be seen that both the conductivity and the permeability have significant influence on the induced voltages of the receiver coil. The peak to peak of the induced voltages are compared in Fig.8. The EMAT obtains maximal transduction efficiency when the core is Mn-Zn ferrite or Ni-Zn ferrite.

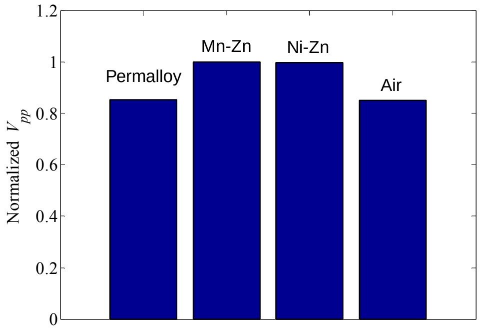

Fig. 8 The peak-to-peak values of induced voltages obtained under cores with different materials.

5. Conclusions

The receiving process of the EMAT for inspection a steel tube by guided waves of longitudinal modes are investigated. A FE mode for simulating the receiving process has been presented based on COMSOL Multiphysics. An optimization about the material of the core in the EMAT has been carried out by using the FE model. This method proposed could also be helpful for the design of the EAMT used as a receiver of other structures.

6. References

1. Kwun, H.,Bartels, K. A. Magnetostrictive sensor technology and its applications. *Ultrasonics*, **36**, 171-178 (1998).

2. Thompson, R. B. A model for the electromagnetic generation of ultrasonic guided waves in ferromagnetic metal polycrystals. *IEEE Trans. Son. Ultrason.*, **25** (1), 7-15 (1978).

3. Sun, P.,Wu, X.,Xu, J. Enhancement of the signal strength for longitudinal guided wave sensors using the magnetic concentrator. *International Journal of Applied Electromagnetics and Mechanics*, **45** (1), 211-217 (2014).

4. Jafari-Shapoorabadi, R.,Konrad, A.,Sinclair, A. N. The governing electrodynamic equations of electromagnetic acoustic transducers. *J. Appl. Phys.*, **97** (10), 10E102 (2005).